

8485

NACA TN 2059

NATIONAL ADVISORY COMMITTEE FOR AERONAUTICS

TECHNICAL NOTE 2059

METHOD OF EXPERIMENTALLY DETERMINING RADIAL DISTRIBUTIONS
OF VELOCITY THROUGH AXIAL-FLOW COMPRESSOR

By Harold B. Finger

Lewis Flight Propulsion Laboratory
Cleveland, Ohio



Washington
April 1950

AFKDO
TECHNICAL NOTE 2059
APR 1950

319.98/41





0065294

NATIONAL ADVISORY COMMITTEE FOR AERONAUTICS

TECHNICAL NOTE 2059

METHOD OF EXPERIMENTALLY DETERMINING RADIAL DISTRIBUTIONS
OF VELOCITY THROUGH AXIAL-FLOW COMPRESSOR

By Harold B. Finger

SUMMARY

A method is presented by which the energy and continuity relations are simultaneously solved to express the velocity distributions downstream of any compressor blade row in terms of outlet total temperature, total pressure, and relative flow angle. The method is intended for use in units in which only a limited amount of experimental data can be obtained. The determination of the velocities downstream of a stationary blade row assumes that the condition of simple radial equilibrium is satisfied and that the entropy is constant along the radius. The method for the rotor requires no such assumption, however, and the effect of the radial displacement of flow passing through the rotor is considered.

INTRODUCTION

The experimental determination and analysis of the performance of a multistage axial-flow compressor requires a knowledge of the radial distribution of flow in the individual components of each stage. Several methods of determining radial distributions of flow downstream of a blade row have previously been devised primarily for design and theoretical studies (references 1 to 3). These methods are not readily applicable to the problem of experimental evaluation of flow distributions in an existing compressor. One of these methods of computing the velocity distribution has been presented in reference 1 and simplified in reference 2. This method, which is based on simple radial equilibrium and incompressible flow, defines the axial-velocity distribution in terms of the absolute tangential-velocity distribution. Reference 3 presents a general method of determining the radial distribution of flow for the compressible case, which considers the radial displacement of flow in passing through a blade row. This general method is also expressed in terms of absolute velocity distributions and absolute flow angles.

Because of instrumentation difficulties and time limitations, however, determination of how fundamental relations can be utilized to define the radial distribution of flow velocities leaving a blade row with a minimum of experimental data is useful. In general, the experimental data required to specify the flow velocities are total temperature, total pressure, static pressure, and absolute flow angle at every point along the radius. The measurement of absolute flow angle and static pressure, however, is extremely difficult. The static pressures and the flow angles must be measured between blade rows in the axial-clearance space, which is usually small and contains turbulent air. The total pressures and the total temperatures can, however, be measured just inside the stator blade rows if no radial shift occurs in the energy distribution. A method of computing velocity distribution downstream of a blade row, based primarily on total-temperature and total-pressure measurements, would therefore be of considerable use in the experimental evaluation of axial-flow-compressor performance. In place of the static pressures and absolute flow angles, which are difficult to measure, however, it would be desirable to use quantities that can be readily determined.

A method was therefore developed at the NACA Lewis laboratory of determining the radial distributions of velocity downstream of a stator and a rotor row of an axial-flow compressor based on a knowledge of total temperature, total pressure, angles of the velocities relative to the blades considered, and total weight flow if axial symmetry can be assumed. The method involves a simultaneous solution of the energy and continuity relations and is considered more applicable than the methods of references 1 to 3 to an existing compressor where a limited amount of experimental data is available. The stator-evaluation method (which is presented in reference 4, but is repeated here for the sake of completeness) assumes that the simple-radial-equilibrium condition is satisfied and that the radial gradient of entropy is negligible. The assumptions eliminate application of the stator method to the determination of the velocities in the boundary-layer regions. The rotor method is general, however, in that it considers the effect of radial displacement of the flow through the rotor row and does not require that the entropy be constant along the radius.

1233

SYMBOLS

The following symbols are used in the calculations:

- c_p specific heat at constant pressure $c_p J g$, ($\text{sq ft}/(\text{°F})(\text{sec}^2)$)
- c_p specific heat at constant pressure, ($\text{Btu}/(\text{lb})(\text{°F})$)
- g acceleration due to gravity, (ft/sec^2)
- P total pressure, (lb/sq ft absolute)
- p static pressure, (lb/sq ft absolute)
- R gas constant for dry air at 59° F , 53.5 ($\text{ft-lb}/(\text{lb})(\text{°R})$)
- r radius, (ft)
- s entropy, ($\text{ft-lb}/(\text{°R})(\text{lb})$)
- T total temperature, (°R)
- t static temperature, (°R)
- U velocity of rotor-blade element ωr , (ft/sec) (fig. 1)
- V absolute air velocity, (ft/sec) (fig. 1)
- V_r radial velocity of air, (ft/sec)
- V_z axial velocity of air, (ft/sec) (fig. 1)
- V_θ tangential velocity of air, (ft/sec) (fig. 1)
- V' velocity of air relative to rotor row, (ft/sec) (fig. 1)
- W weight flow, (lb/sec)
- z axial distance, (ft)
- β angle between absolute air velocity and axial direction, (deg) (fig. 1)
- β' angle between relative air velocity and axial direction, (deg) (fig. 1)

- δ boundary-layer displacement thickness, (ft)
- γ isentropic exponent
- ρ static density, (slugs/cu ft)
- ω angular velocity of rotor, (radians/sec)

Subscripts:

- 1 inlet to rotor
- 2 outlet from rotor
- 3 outlet from stator
- h hub
- t tip
- x any specified radial location used as reference point

ANALYSIS

The following analysis develops a method of determining the velocity distributions in an axial-flow-compressor stage such as that shown in figure 2, which is based on a knowledge of total temperatures, total pressures, relative flow angles, and total weight flow. The total temperatures and the total pressures should be measured in the axial-clearance space or, if the clearance is too small, inside each stator row if the instruments are properly aligned with the flow. A representation of circumferential variations should be obtained to determine if the condition of axial symmetry is satisfied. The relative flow angles from each blade row can be estimated by application of stationary cascade investigations and empirical rules based on cascade investigations with corrections applied for compressibility and induced velocity effects. If the absolute flow angles at the outlet from each blade row can be experimentally measured, the general method of reference 3 or the stator-evaluation method presented herein, which may be considered as based on absolute flow angles, can be applied to determine the radial distribution of flow downstream of each stator or rotor row. The difficulties involved in instrumentation and the requirement that instrumentation effects be kept small, however, necessitate the use of only those instruments that are essential.

to the determination of the velocity distributions. For this reason and because the accurate measurement of absolute flow angle and static pressure is difficult, a method of determining the axial-velocity distribution downstream of a rotor row in terms of the relative flow angle and easily measured quantities is required. When the axial velocities and flow angles are known, the complete velocity diagram can be constructed.

Velocity distribution downstream of stator row. - The following discussion presents the derivation of the method (previously presented in reference 4) of determining the velocity distribution downstream of a stationary blade row, guide vanes or stators, if total temperatures, total pressures, and flow angles are known. The development assumes that the simple-radial-equilibrium condition is satisfied and that the entropy is constant along the radius downstream of the blade row.

The energy equation for adiabatic compressible flow can be stated as:

$$t_3 = T_3 - \frac{v_{\theta,3}^2}{2C_p} - \frac{v_{z,3}^2}{2C_p} - \frac{v_{r,3}^2}{2C_p} \quad (1)$$

Differentiation with respect to the radius gives

$$\frac{dt_3}{dr_3} = \frac{dT_3}{dr_3} - \frac{1}{2C_p} \frac{d(v_{\theta,3}^2)}{dr_3} - \frac{1}{2C_p} \frac{d(v_{z,3}^2)}{dr_3} - \frac{1}{2C_p} \frac{d(v_{r,3}^2)}{dr_3} \quad (2)$$

The fundamental relation for the variation of entropy with radius is given by

$$t_3 \frac{ds_3}{dr_3} = C_p \frac{dt_3}{dr_3} - \frac{1}{\rho_3} \frac{dp_3}{dr_3}$$

If constant entropy along the radius is assumed,

$$\frac{dt_3}{dr_3} = \frac{1}{C_p \rho_3} \frac{dp_3}{dr_3} \quad (3)$$

Substitution of equation (3) into equation (2) gives

$$\frac{1}{C_p \rho_3} \frac{dp_3}{dr_3} = \left[\frac{dT_3}{dr_3} - \frac{1}{2C_p} \frac{d(v_{\theta,3}^2)}{dr_3} - \frac{1}{2C_p} \frac{d(v_z^2)}{dr_3} - \frac{1}{2C_p} \frac{d(v_r^2)}{dr_3} \right] \quad (4)$$

For radial equilibrium,

$$\frac{1}{\rho_3} \frac{dp_3}{dr_3} = \frac{v_{\theta,3}^2}{r_3} - v_{r,3} \frac{\partial v_{r,3}}{\partial r_3} - v_{z,3} \frac{\partial v_{r,3}}{\partial z_3}$$

If the assumption is made that v_r or $\partial v_r / \partial r$ and $\partial v_r / \partial z = 0$

$$\frac{1}{\rho_3} \frac{dp_3}{dr_3} = \frac{v_{\theta,3}^2}{r_3} \quad (5)$$

When $v_r = 0$, equations (4) and (5) combine to yield

$$\frac{dT_3}{dr_3} - \frac{1}{2C_p} \frac{d(v_{\theta,3}^2)}{dr_3} - \frac{1}{2C_p} \frac{d(v_z^2)}{dr_3} - \frac{1}{C_p} \frac{v_{\theta,3}^2}{r_3} = 0 \quad (6)$$

Equation (6) expresses the exact relation between the gas velocities and the gas state where radial velocities and their gradients are negligible, and when the gradient of entropy along the radius is zero.

From vector-diagram considerations (fig. 1)

$$v_{\theta,3} = v_{z,3} \tan \beta_3 \quad (7)$$

Equation (6) therefore becomes

$$\frac{dT_3}{dr_3} - \frac{1}{2C_p} \frac{d(v_{z,3}^2 \tan^2 \beta_3)}{dr_3} - \frac{1}{2C_p} \frac{d(v_z^2)}{dr_3} - \frac{1}{C_p} \frac{v_{z,3}^2 \tan^2 \beta_3}{r_3} = 0$$

Collecting terms and performing the indicated operations gives

$$\frac{dT_3}{dr_3} - \frac{1}{2C_p} \left[v_{z,3}^2 \left(2 \tan \beta_3 \sec^2 \beta_3 \frac{d\beta_3}{dr_3} + \frac{2 \tan^2 \beta_3}{r_3} \right) + \frac{d(v_{z,3}^2)}{dr_3} \sec^2 \beta_3 \right] = 0$$

Division by $\sec^2 \beta_3$, multiplication, and rearrangement of terms gives

$$2C_p \frac{dT_3}{dr_3} \frac{1}{\sec^2 \beta_3} = v_{z,3}^2 \left(2 \tan \beta_3 \frac{d\beta_3}{dr_3} + \frac{2 \sin^2 \beta_3}{r_3} \right) + \frac{d(v_{z,3}^2)}{dr_3}$$
(8)

If

$$S = \left(2 \tan \beta_3 \frac{d\beta_3}{dr_3} + \frac{2 \sin^2 \beta_3}{r_3} \right)$$

and

$$Q = 2C_p \frac{dT_3}{dr_3} \frac{1}{\sec^2 \beta_3}$$

equation (8) can be written as

$$S(v_{z,3}^2) dr_3 + d(v_{z,3}^2) = Q dr_3$$

which is a first-order differential equation linear in v_z^2 that has the following solution:

$$\left[v_{z,3}^2 \exp \left(\int_{r_x}^r S dr_3 \right) \right]_{r_x}^r = \int_{r_x}^r Q \exp \left(\int_{r_x}^r S dr_3 \right) dr_3$$

If the values of S and Q are substituted

$$\left\{ V_{z,3}^2 \exp \left[\int_{r_x}^r \left(2 \tan \beta_3 \frac{d\beta_3}{dr_3} + \frac{2 \sin^2 \beta_3}{r_3} \right) dr_3 \right] \right\}_{r_x}^r \\ = \int_{T_{3,x}}^{T_3} \frac{2C_p}{\sec^2 \beta_3} \exp \left[\int_{r_x}^r \left(2 \tan \beta_3 \frac{d\beta_3}{dr_3} + \frac{2 \sin^2 \beta_3}{r_3} \right) dr_3 \right] dT_3 \quad (9)$$

The exponential in equation (9) can be evaluated as follows:

$$\int_{r_x}^r \left(2 \tan \beta_3 \frac{d\beta_3}{dr_3} + \frac{2 \sin^2 \beta_3}{r_3} \right) dr_3 = \int_{r_x}^r \frac{2 \sin^2 \beta_3}{r_3} dr_3 + \\ 2 \log_e \left(\frac{\cos \beta_{3,x}}{\cos \beta_3} \right)$$

Therefore

$$\exp \left[\int_{r_x}^r 2 \left(\tan \beta_3 \frac{d\beta_3}{dr_3} + \frac{\sin^2 \beta_3}{r_3} \right) dr_3 \right] \\ = \left(\frac{\cos \beta_{3,x}}{\cos \beta_3} \right)^2 \exp \left(\int_{r_x}^r \frac{2 \sin^2 \beta_3}{r_3} dr_3 \right) \quad (10)$$

By application of equation (10), equation (9) reduces to

$$\begin{aligned} & \left[v_{z,3}^2 \left(\frac{\cos \beta_{3,x}}{\cos \beta_3} \right)^2 \exp \left(\int_{r_x}^r \frac{2 \sin^2 \beta_3}{r_3} dr_3 \right) \right]_x^r \\ &= \int_{T_{3,x}}^{T_3} \frac{2C_p}{\sec^2 \beta_3} \left(\frac{\cos \beta_{3,x}}{\cos \beta_3} \right)^2 \left[\exp \left(\int_{r_x}^r \frac{2 \sin^2 \beta_3}{r_3} dr_3 \right) \right] dT_3 \end{aligned}$$

Evaluation over the limits indicated gives

$$\begin{aligned} & v_{z,3}^2 \left(\frac{\cos \beta_{3,x}}{\cos \beta_3} \right)^2 \exp \left(\int_{r_x}^r \frac{2 \sin^2 \beta_3}{r_3} dr_3 \right) - v_{z,3,x}^2 \\ &= \int_{T_{3,x}}^{T_3} 2C_p \cos^2 \beta_{3,x} \exp \left(\int_{r_x}^r \frac{2 \sin^2 \beta_3}{r_3} dr_3 \right) dT_3 \quad (11) \end{aligned}$$

Transposition of terms gives

$$\begin{aligned} v_{z,3}^2 &= \frac{\int_{T_{3,x}}^{T_3} 2C_p \cos^2 \beta_{3,x} \exp \left(\int_{r_x}^r \frac{2 \sin^2 \beta_3}{r_3} dr_3 \right) dT_3}{\left(\frac{\cos \beta_{3,x}}{\cos \beta_3} \right)^2 \exp \left(\int_{r_x}^r \frac{2 \sin^2 \beta_3}{r_3} dr_3 \right)} + \\ &\quad \frac{v_{z,3,x}^2}{\left(\frac{\cos \beta_{3,x}}{\cos \beta_3} \right)^2 \exp \left(\int_{r_x}^r \frac{2 \sin^2 \beta_3}{r_3} dr_3 \right)} \quad (12) \end{aligned}$$

If the total temperature is constant along the radius as is the case downstream of the compressor-inlet guide vanes, equation (12) reduces to

$$V_{z,3} = \frac{V_{z,3,x}}{\left(\frac{\cos \beta_{3,x}}{\cos \beta_3} \right) \exp \left(\int_{r_x}^r \frac{\sin^2 \beta_3}{r_3} dr_3 \right)} \quad (13)$$

From the continuity equation

$$W = \int_{r_h}^{r_t} 2\pi r \rho g V_z dr = \int_{r_h^2}^{r_t^2} \pi \rho g V_z d(r^2) \quad (14)$$

Equation (14) as stated does not include the effects of annulus-wall boundary layers and blade wakes in reducing the effective flow area. Because the calculation for V_z is based on the assumption that the radial gradient of entropy is negligible, the low-energy regions of the boundary layer must be omitted from consideration. Because the weight flow transported by the boundary layer is comparatively small, the effect of the wall boundary layers on the velocities over most of the passage, however, can be considered by adding and subtracting the boundary-layer displacement thickness from the lower and upper limits, respectively, of equation (14). Thus the limits of integration would be $(r_t - \delta_t)$ and $(r_h + \delta_h)$ or $(r_t - \delta_t)^2$ and $(r_h + \delta_h)^2$. In effect, this change in limits alters the annulus dimensions to an equivalent annulus area in which the thickness of wall boundary layer is negligible. The equivalent annulus dimensions must then also be used in equations (12) and (13). The effect of blade wakes can be considered by inserting a multiplying factor in equation (14), which will in effect subtract the wake thickness from the annulus-area term. The minimum effect of wake thickness can be obtained by assuming that the wake has the same thickness as the blade trailing edge.

1233

Equations (12) or (13) and (14) can then be simultaneously solved by an iteration process with the isentropic relation for density given as

$$\rho = \frac{P}{gRT} \left(1 - \frac{\gamma-1}{2} \frac{\frac{V_z^2}{2}}{\gamma gRT \cos \beta} \right)^{\frac{1}{\gamma-1}} \quad (15)$$

The three unknowns in these equations are $V_{z,x}$, V_z , and ρ .

The method thus developed determines the velocity distribution downstream of a stator-blade row if the total pressure, total temperature, air-weight flow, and flow angle are known for the case where the simple-radial-equilibrium condition is satisfied and the entropy is constant along the radius. If the method is to be applied to a nozzle row operating at supercritical pressure ratios, special care must be taken to obtain the true relative flow angle. At supercritical pressure ratios, the effect of jet deflection on flow angle must be considered.

Velocity distribution downstream of rotor row. - The following discussion presents the development of a method of determining the radial distribution of velocity downstream of a rotor row in terms of the rotor-outlet total temperature, total pressure, relative flow angle, and rotor-inlet conditions.

The general energy equation for adiabatic relative flow across any rotor blade row can be written as

$$c_p t_1 + \frac{(v'_2)^2}{2} - \frac{\omega^2 r_1^2}{2} = c_p t_2 + \frac{(v'_2)^2}{2} - \frac{\omega^2 r_2^2}{2} \quad (16)$$

From vector-diagram considerations (fig. 1), the relative velocity is given by

$$(v')^2 = v^2 - u^2 + 2uv_z \tan \beta \quad (17)$$

If equations (16) and (17) are combined and because

$$C_p t + \frac{1}{2} V^2 = C_p T,$$

$$\frac{1}{U_2} \left[C_p (T_1 - T_2) - (U_1^2 - U_2^2) + U_1 V_{z,1} \tan \beta'_1 \right] = V_{z,2} \tan \beta'_2$$
(18)

Differentiation of equation (18) with respect to r_2 and division by $\tan \beta'_2$ yields

$$\begin{aligned} & \frac{1}{\tan \beta'_2} \frac{d}{dr_2} \left\{ \frac{1}{U_2} \left[C_p (T_1 - T_2) - (U_1^2 - U_2^2) + U_1 V_{z,1} \tan \beta'_1 \right] \right\} \\ &= \frac{V_{z,2}}{\sin \beta'_2 \cos \beta'_2} \frac{d\beta'_2}{dr_2} + \frac{dV_{z,2}}{dr_2} \end{aligned} \quad (19)$$

All terms in the left side of equation (19) can be readily determined by actual measurement or computation as a function of radius. The values of $(T_1 - T_2)$ and $(U_1^2 - U_2^2)$, however, depend on the radial displacement of flow through the rotor row because these difference terms require that the measurements be made on the same streamline. As a first approximation, the displacement can be assumed. The actual displacement will be determined later in the development.

At any radius, let

$$Q = \frac{1}{\tan \beta'_2} \frac{d}{dr_2} \left\{ \frac{1}{U_2} \left[C_p (T_1 - T_2) - (U_1^2 - U_2^2) + U_1 V_{z,1} \tan \beta'_1 \right] \right\}$$

and

$$S = \frac{1}{\sin \beta'_2 \cos \beta'_2} \frac{d\beta'_2}{dr_2}$$

1233

Equation (19) can then be written as

$$Q = SV_{z,2} + \frac{dV_{z,2}}{dr_2}$$

which is a first-order differential equation linear in V_z , which has the solution

$$\left[V_{z,2} \exp\left(\int S dr_2\right) \right]_{r_x}^r = \int_{r_x}^r Q \exp\left(\int S dr_2\right) dr_2 \quad (20)$$

The integral, which is the exponent of e in equation (20), is taken over the limits r_x to r and can be evaluated as follows:

$$\int_{r_x}^r S dr_2 = \int_{r_x}^r \frac{dr_2}{\sin \beta'_{2,x} \cos \beta'_{2,x}} \frac{d\beta'_{2,x}}{dr_2} = \log_e \frac{\tan \beta'_{2,x}}{\tan \beta'_{2,r}}$$

Therefore

$$\exp\left(\int_{r_x}^r S dr_2\right) = \frac{\tan \beta'_{2,x}}{\tan \beta'_{2,r}}$$

Equation (20) then becomes

$$V_{z,2} \frac{\tan \beta'_{2,x}}{\tan \beta'_{2,r}} - V_{z,2,r} = \int_{r_x}^r Q \frac{\tan \beta'_{2,x}}{\tan \beta'_{2,r}} dr_2$$

Integration as indicated and substitution of the expression for Q gives

$$\begin{aligned} & V_{z,2} \frac{\tan \beta'_{2,x}}{\tan \beta'_{2,r}} - V_{z,2,r} \\ &= \frac{1}{\tan \beta'_{2,r}} \left\{ \frac{1}{U_2} \left[C_p (T_1 - T_2) - (U_1^2 - U_2^2) + U_1 V_{z,1} \tan \beta'_{1,x} \right] \right\}_{r_x}^r \end{aligned}$$

or

$$\frac{V_{z,2}}{V_{z,2,x}} = \frac{\tan \beta'_{2,x}}{\tan \beta'_{2}} + \frac{1}{V_{z,2,x} \tan \beta'_{2}} \left\{ \frac{1}{U_2} \left[C_p (T_1 - T_2) - (U_1^2 - U_2^2) + \right. \right. \\ \left. \left. U_1 V_{z,1} \tan \beta'_{1} \right] \right\}_{r_x}^r \quad (21)$$

The continuity equation can be written as

$$W = \int_{r_{1,h}}^{r_{1,t}} 2\pi r_1 \rho_1 g V_{z,1} dr_1 = \int_{r_{2,h}}^{r_{2,t}} 2\pi r_2 \rho_2 g V_{z,2,x} \left(\frac{V_{z,2}}{V_{z,2,x}} \right) dr_2 \quad (22)$$

Substitution of equation (21) into the continuity relation equation (22) gives

$$W = \int_{r_{2,h}}^{r_{2,t}} \frac{2\pi r_2 \rho_2 g}{\tan \beta'_{2}} \left\{ \frac{1}{U_2} \left[C_p (T_1 - T_2) - (U_1^2 - U_2^2) + \right. \right. \\ \left. \left. U_1 V_{z,1} \tan \beta'_{1} \right] \right\}_{r_x}^r dr_2 + V_{z,2,x} \int_{r_{2,h}}^{r_{2,t}} 2\pi r_2 \rho_2 g \frac{\tan \beta'_{2,x}}{\tan \beta'_{2}} dr_2 \quad (23)$$

which can be solved for $V_{z,2,x}$ for any weight flow by graphical or numerical integration for the assumed distribution of density at the rotor outlet and for the assumed radial displacement. An axial-velocity distribution can then be determined from equation (21). As in the stator method, the continuity relation (22) should be

corrected to consider the effect of boundary layer and blade wakes. Just as in the stator analysis, changing the integration limits by an amount equal to the boundary-layer displacement thickness and inserting a multiplication factor in the continuity relation are probably the simplest means of considering the effects of these low-energy regions on the effective annular flow area. If complete survey data are available in the boundary-layer and wake regions, the relations can be used as presented because it has not been necessary to assume negligible gradient of entropy along the radius. The effect of the wakes may actually be indirectly considered if the measurements are made far enough downstream of the rotor so that the wakes have been dissipated.

The distributions of velocity, density, and radial displacements are determined by a trial-and-error solution of equations (21), (23), the continuity relation, and the definition of static density given as

$$\rho_2 = \frac{P_2}{gRT_2^2} \left(1 - \frac{\gamma-1}{2} \frac{V_{z,2}^2}{\gamma gRT_2 \cos^2 \beta_2} \right)^{\frac{1}{\gamma-1}} \quad (24)$$

The four unknowns in these relations are $V_{z,2,x}$, $V_{z,2}$, ρ_2 , and the radial displacement of flow passing through the rotor, which enters in the $(U_1^2 - U_2^2)$ and $(T_1 - T_2)$ terms. The continuity relation used in this trial-and-error solution states that the mass flow between any two stream surfaces is constant all along the length of the streamlines; that is,

$$\rho_1 V_{z,1} r_1 dr_1 = \rho_2 V_{z,2} r_2 dr_2 \quad (25)$$

APPLICATION OF METHOD

Apparatus and Instrumentation

The method of determining the velocity distribution at the outlet of the rotor and stator rows if total temperatures, total pressures, and relative flow angles throughout the compressor are known has been used to calculate the velocity distributions in a 10-stage

axial-flow compressor. In addition to over-all instrumentation, located as described in reference 5, the compressor was so instrumented that the total temperatures and pressures at three radial positions and three circumferential positions could be determined midway between the leading and trailing edges of the blades in each stator row (fig. 2). Although the measurements were made within the stator row, it was assumed that the total-pressure and total-temperature distributions at the inlet and outlet of the blade row were the same as those indicated by the instruments. That is, viscous and heat-transfer losses and radial shift in the energy distribution were assumed to be small in the stator. Outer-wall static-pressure measurements were made upstream and downstream of each blade row and were used as an indication of the accuracy of the computations.

Stator Method

The determination of the velocity distribution downstream of a stationary blade row if the total temperatures, total pressures, relative flow angles, and air-weight flow are known requires the simultaneous solution of the following relations:

$$v_{z,3}^2 = \frac{\int_{T_{3,x}}^{T_3} 2C_p \cos^2 \beta_{3,x} \exp\left(\int_{r_x}^r \frac{2 \sin^2 \beta_3}{r_3} dr_3\right) dT_3}{\left(\frac{\cos \beta_{3,x}}{\cos \beta_3}\right)^2 \exp\left(\int_{r_x}^r \frac{2 \sin^2 \beta_3}{r_3} dr_3\right)} + \frac{v_{z,3,x}^2}{\left(\frac{\cos \beta_{3,x}}{\cos \beta_3}\right)^2 \exp\left(\int_{r_x}^r \frac{2 \sin^2 \beta_3}{r_3} dr_3\right)} \quad (12)$$

$$W = \int_{r_h}^{r_t} 2\pi r \rho g v_z dr = \int_{r_h}^{r_t} \pi \rho g v_z d(r^2) \quad (14)$$

and

$$\rho = \frac{P}{gRT} \left(1 - \frac{\gamma-1}{2} \frac{V_z^2}{\gamma gRT \cos^2 \beta} \right)^{\frac{1}{\gamma-1}} \quad (15)$$

In the present application, the total temperatures, total pressures, and weight flow were experimentally measured and the flow angles were determined using Constant's rule (reference 6) with revision for the effect of blade stagger on flow angle. Thus, the unknowns in the three equations are $V_{z,x}$, V_z , and ρ .

As a preliminary step in the calculation procedure, a radial distribution of static density (constant density is the simplest assumption with which to start) must be assumed. The relation for $V_{z,3}$ determined by inserting the known distributions of total temperature and flow angle into equation (12) can then be substituted into equation (14). It should be noted again that the effect of wall boundary layers and blade wakes on equation (14) can be considered by changing the limits of integration and inserting a multiplication factor as discussed in the ANALYSIS. If the known weight flow and the assumed density distribution are used, equations (12) and (14) can be simultaneously solved for $V_{z,3,x}$ by a trial-and-error procedure. Several values of $V_{z,3,x}$ can be assumed until the integration checks the known weight flow. It is generally sufficient to make two or three assumptions of $V_{z,3,x}$ and interpolate between them. The value of $V_{z,3,x}$ determined for the assumed density distribution can therefore be substituted into equation (12) and a radial distribution of axial velocity can be computed. When this distribution of axial velocity is used, a new distribution of static density can be determined by equation (15). The process is then repeated with the new distribution of density. Usually, only two or three trials are necessary until the final density distribution checks the one used in the continuity relation (equation (14)).

In the calculation of the velocities downstream of the third stator of the 10-stage compressor at the peak efficiency point at the design speed, the wall boundary layers were first assumed negligible and then the displacement thickness of the boundary layer was assumed to be 0.10 inch on both the inner and outer walls. In the first case, equation (14) was used as stated and in the second

case, the limits of integration in equation (14) were adjusted by use of the displacement thickness. The axial-velocity distributions determined for both conditions are presented in figure 3(a). The effect of wake thickness has been neglected in this calculation. The velocity distributions for the two boundary-layer conditions have the same general shape. The axial-velocity distribution when the effect of the 0.10-inch boundary-layer displacement thickness is considered, however, gives higher velocities than the curve for which the boundary layer has been neglected. At the midsection, the difference in velocities is approximately 5.5 percent. As an indication of the accuracy of the method, the calculated static-pressure distribution is compared with the measured wall static pressure in figure 3(b). On the basis of these limited data, it is seen that the difference between the measured and calculated static pressure at the outer wall is approximately 3 percent when the boundary layer is neglected and approximately 1 percent when a boundary-layer displacement thickness of 0.10 inch is assumed.

Rotor Method

The evaluation of the velocities downstream of the rotor row, which assumes a knowledge of total temperature, total pressure, and relative flow angles downstream of the blade row as well as the flow conditions upstream of the row is based on a simultaneous solution of the following relations:

$$\frac{V_{z,2}}{V_{z,2,x}} = \frac{\tan \beta'_{2,x}}{\tan \beta'_{2}} + \frac{1}{V_{z,2,x} \tan \beta'} \left\{ \frac{1}{U_2} \left[C_p (T_1 - T_2) - (U_1^2 - U_2^2) + U_1 V_{z,1} \tan \beta'_{1} \right] \right\}_{r_x}^r$$

(21)

$$W = \int_{r_{2,h}}^{r_{2,t}} \frac{2\pi r_2 \rho_2 g}{\tan \beta'_2} \left\{ \frac{1}{U_2} \left[C_p (T_1 - T_2) - (U_1^2 - U_2^2) + U_1 V_{z,1} \tan \beta'_1 \right] \right\} \frac{r}{r_x} dr_2 +$$

$$V_{z,2,x} \int_{r_{2,h}}^{r_{2,t}} 2\pi r_2 \rho_2 g \frac{\tan \beta'_2}{\tan \beta'_2} dr_2 \quad (23)$$

$$\rho_2 = \frac{P_2}{gRT_2} \left(1 - \frac{\gamma-1}{2} \frac{V_{z,2}^2}{\gamma gRT_2 \cos^2 \beta_2} \right)^{\frac{1}{\gamma-1}} \quad (24)$$

and

$$\rho_1 V_{z,1} r_1 dr_1 = \rho_2 V_{z,2} r_2 dr_2 \quad (25)$$

The relative flow angles at the rotor outlet in this investigation were determined from the revised empirical rule of Constant (reference 6). The stator evaluation method presented herein was used to determine the velocity distribution at the inlet to the rotor row. Thus, the unknowns in the previous equations are $V_{z,2}$, $V_{z,2,x}$, ρ_2 , and r_2/r_1 .

As the preliminary step of the calculation procedure, it is necessary to assume the radial distribution of ρ_2 and r_2/r_1 . The r_2/r_1 term represents the radial displacement of the flow passing through the rotor row. In this case, the density and the radial-displacement distributions were assumed for each weight flow and rotor speed investigated so that equation (23) could be used to determine the first trial value of $V_{z,2,x}$. Substitution of this value of $V_{z,2,x}$ into equation (21) with the assumed value of radial

displacement, which enters as the $(U_1^2 - U_2^2)$ and $(T_1 - T_2)$ terms, determines a radial distribution of axial velocity. A new distribution of density can then be determined using equation (24) with the known values of total temperature and pressure and the absolute velocities, which are computed from axial velocity (determined from equation (21)), relative flow angle, and blade speed. By using this new density distribution and the previously computed axial-velocity distribution, the rotor-outlet annulus and the inlet-annulus areas are divided into equal mass-flow increments such that a new radial displacement is determined; that is, equation (25) is mechanically integrated to obtain a new distribution of r_2/r_1 . Division of the inlet and the outlet annulus areas into equal flow increments determines the positions of several streamlines at the inlet and the outlet of the rotor and therefore determines the radial displacement of flow. This new displacement and the density distribution determined from equation (24) are then resubstituted into equation (23) to determine the second trial value of $V_{z,2,x}$. The entire process is then repeated until the density and the radial displacement are constant in each further trial. Two or three trials are generally all that are required to obtain convergence.

The axial-velocity distribution at the outlet of the fourth rotor row of the 10-stage compressor is presented in figure 4(a) for several boundary-layer configurations. It can be seen that the curves have the same shape over most of the passage with an over-all difference of approximately 4 percent. The over-all difference becomes large in the vicinity of the hub reaching approximately 40 percent near the wall. The differences between the two curves when boundary-layer thickness is considered result from the effect of the differences in the velocity and angle distributions at the rotor inlet.

In figure 4(b), is presented the comparison between the measured and calculated wall static pressures downstream of the fourth rotor row for the three boundary-layer conditions considered. The three curves are practically coincident over the central portion of the passage. The difference between the calculated and measured wall pressure is approximately 3 percent. As was the case in the stator calculation, the effect of blade wakes on velocity distribution has been neglected in determining the results of figure 4. The wakes have been considered indirectly, however, because the measurements used in these rotor calculations were made downstream of the rotor where the wakes have probably been dissipated and where average conditions have been indicated. An error introduced in the present calculations is the effect of possible errors in relative flow angle. As an indication of the effect of flow angle on the rotor results,

1233

an error of 2° would cause a maximum error of approximately 1.5 percent in the axial velocities calculated.

CONCLUDING REMARKS

A method is presented for determining the velocity distributions downstream of any compressor blade row in terms of outlet total temperature, total pressure, and relative flow angle. The method is intended for use in units in which only a limited amount of experimental data can be obtained. The determination of the velocities downstream of a stationary blade row assumes that the condition of simple radial equilibrium is satisfied and that the entropy is constant along the radius. The method for the rotor makes no such assumption, however, and considers the effect of the radial displacement of flow passing through the rotor. The application of the method to the determination of the velocities and pressures in a 10-stage compressor has indicated good agreement with the measured wall-static pressures.

Lewis Flight Propulsion Laboratory,
National Advisory Committee for Aeronautics,
Cleveland, Ohio, October 13, 1949.

REFERENCES

1. Ruden, P.: Investigation of Single Stage Axial Fans.
NACA TM 1062, 1944.
2. Kahane, A.: Investigation of Axial-Flow Fan and Compressor Rotors Designed for Three-Dimensional Flow. NACA TN 1652, 1948.
3. Wu, Chung-Hua, and Wolfenstein, Lincoln: Application of Radial-Equilibrium Condition to Axial-Flow Compressor and Turbine Design. NACA TN 1795, 1949.
4. Finger, Harold B., Schum, Harold J., and Buckner, Howard A., Jr.: Experimental and Theoretical Distribution of Flow Produced by Inlet Guide Vanes of an Axial-Flow Compressor. NACA TN 1954, 1949.
5. NACA Subcommittee on Compressors: Standard Procedures for Rating and Testing Multistage Axial-Flow Compressors. NACA TN 1138, 1946.
6. Constant, H.: Note on Performance of Cascades of Aerofoils.
Rep. No. E.3696, British R.A.E., June 1939.

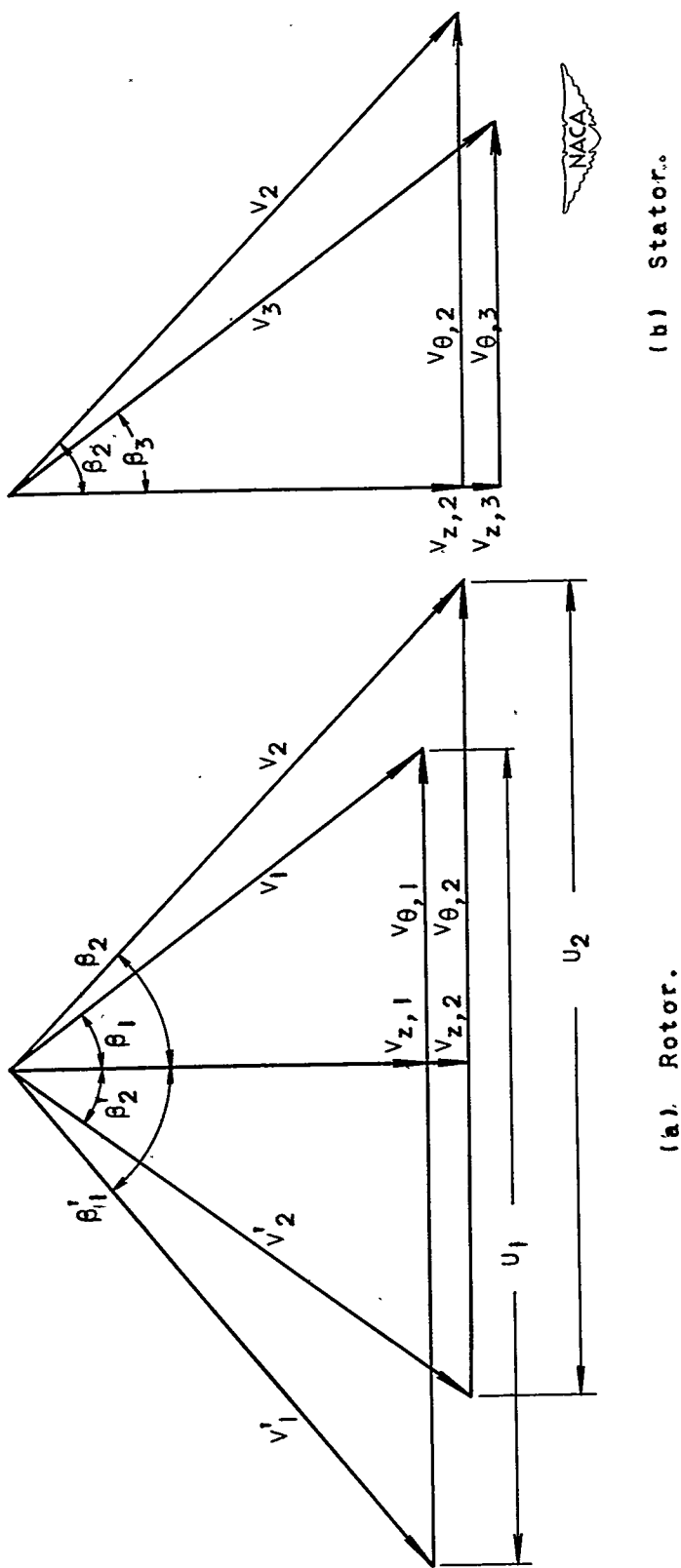


Figure 1. — Vector diagram for axial-flow compressor stage.

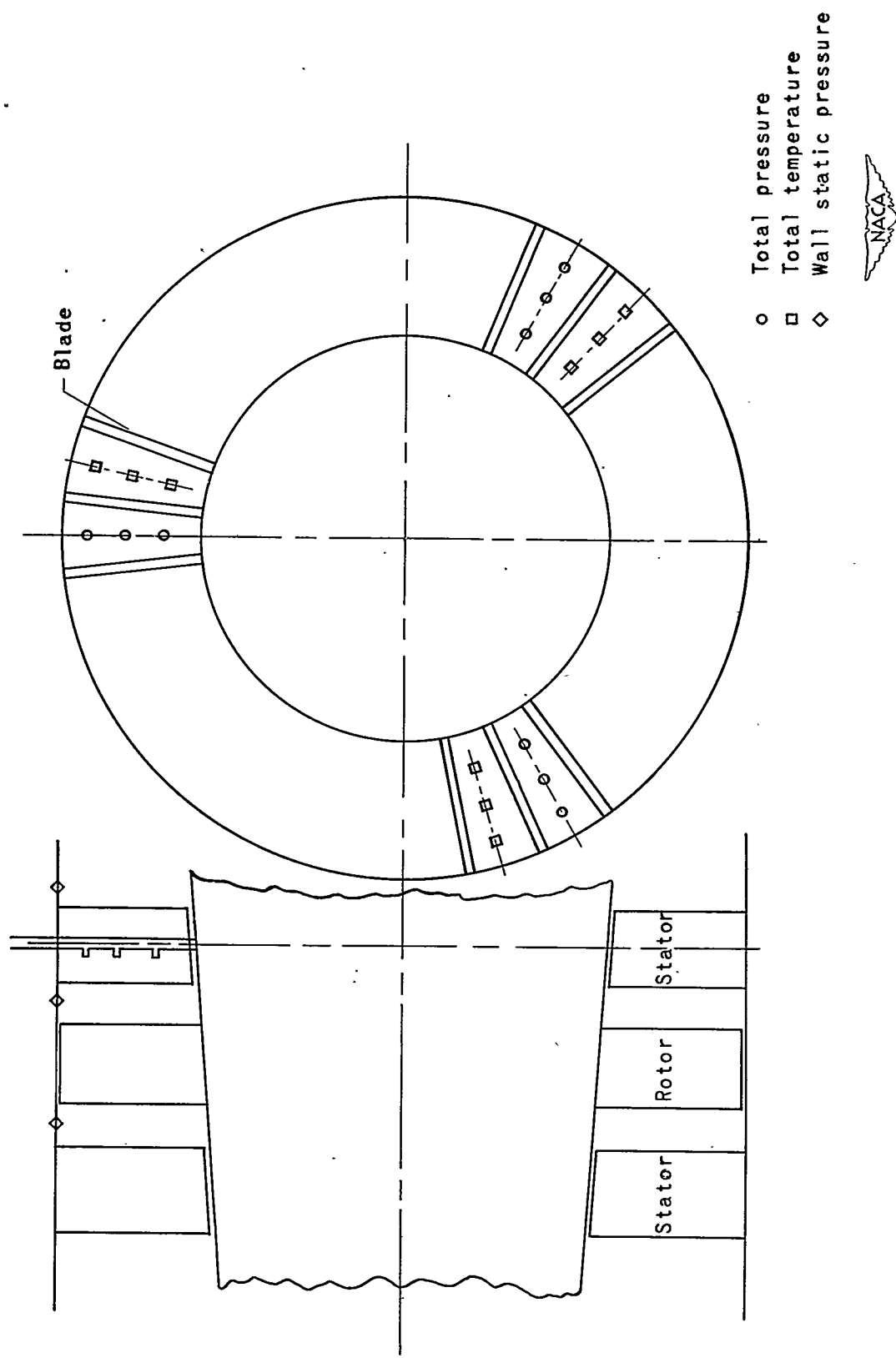


Figure 2. — Schematic diagram of interstage instrumentation.

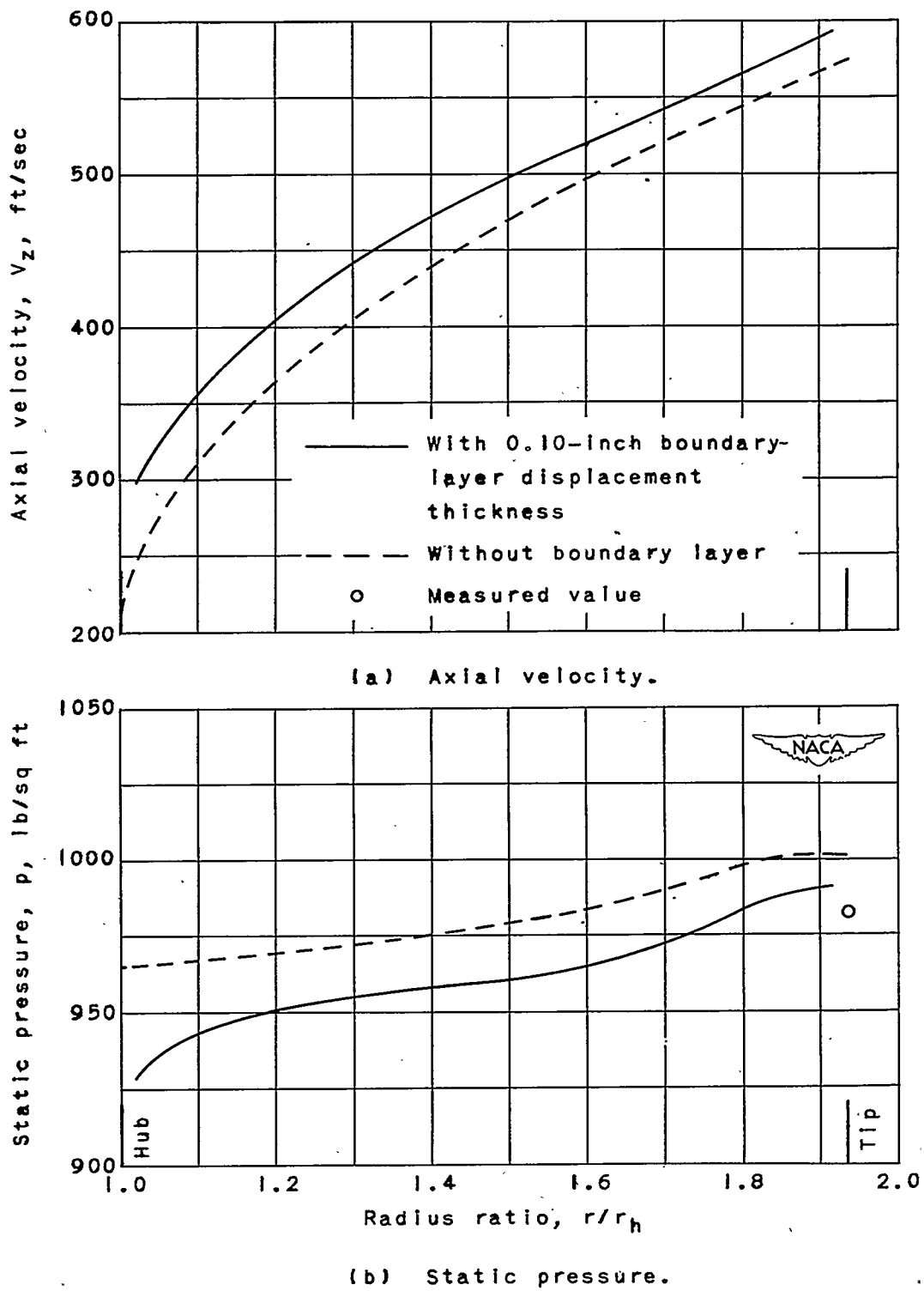


Figure 3. -- Radial distribution of axial velocity and static pressure downstream of third stator row.

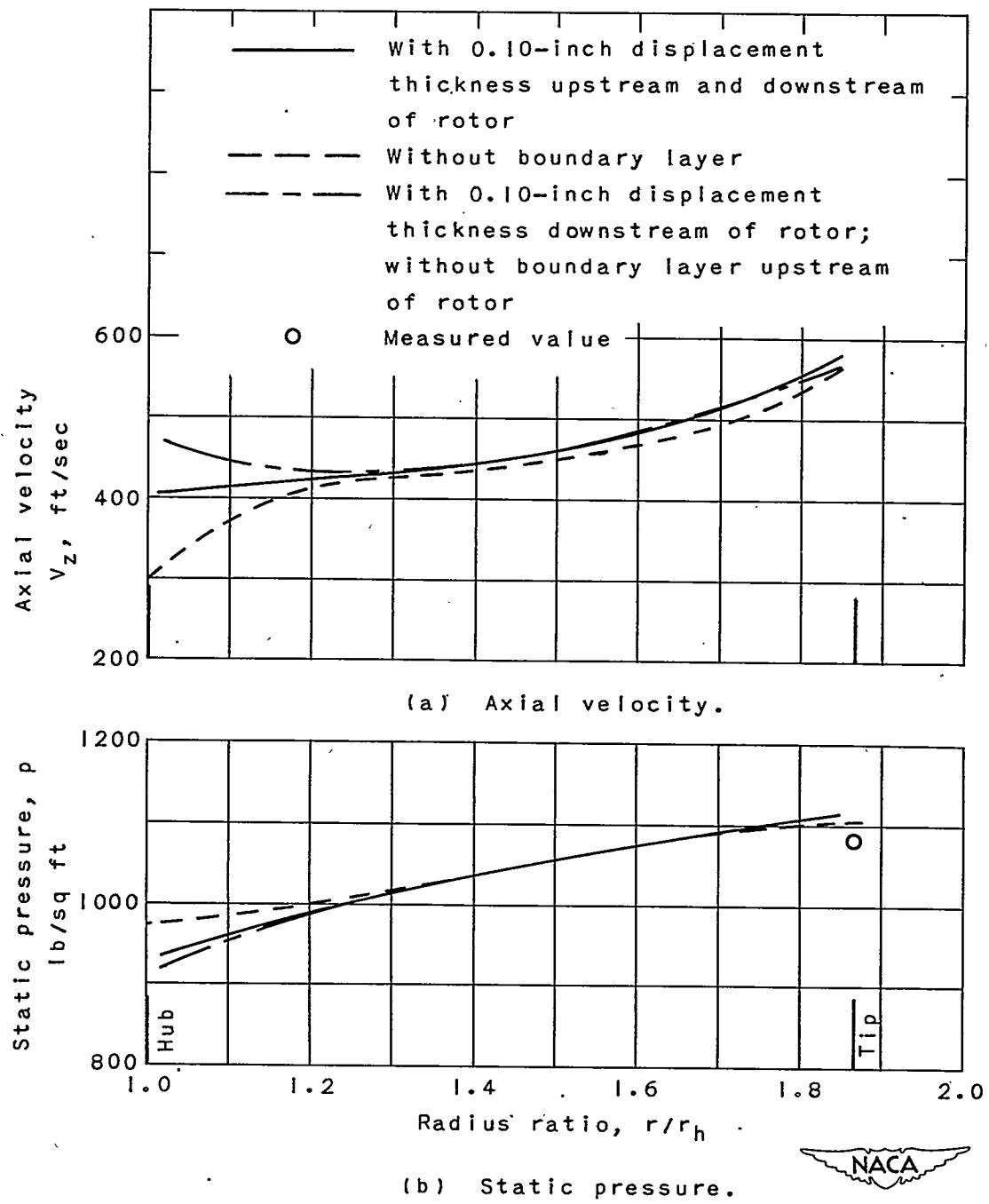


Figure 4. - Radial distribution of axial velocity and static pressure downstream of fourth rotor row.